

# Computational NMR of the iron pyrazolylborate complexes $[\text{Tp}_2\text{Fe}]^+$ and $\text{Tp}_2\text{Fe}$ including solvation and spin-crossover effects

Ari Pyykkönen and Juha Vaara\*

*NMR Research Unit, University of Oulu, P.O. Box 3000, Oulu FIN-90014, Finland*

## Electronic Supplementary Information

### Contents

Optimised geometries	2
Reference shieldings	13
Zero-field splitting parameters	13
Full numerical pNMR results for $[\text{Tp}_2\text{Fe}]^+$	14
Temperature series of $[\text{Tp}_2\text{Fe}]^+$	15
Excited state of $[\text{Tp}_2\text{Fe}]^+$	16
Physical contributions to the isotropic nuclear shieldings	18
Full numerical pNMR results for $\text{Tp}_2\text{Fe}$	23
NMR shifts with alternative experimental $\Delta H$ and $\Delta S$ (Ref. <sup>1</sup> ) for $\text{Tp}_2\text{Fe}$	25
Energetics of the spin-crossover system $\text{Tp}_2\text{Fe}$	26

# Optimised geometries

All coordinates given in xyz format in Å.

Table ESI1: Structure of  $[\text{Tp}_2\text{Fe}]^+$  from an unconstrained ground-state optimisation.

---

53			
Fe	-0.0015735	0.0031380	-0.0012445
B	-1.7434811	-1.6442560	-1.9152690
B	1.7430294	1.6416123	1.9179125
C	0.5267063	-2.9036487	0.5847459
C	2.8629863	-0.7385992	-0.5602747
C	4.1242633	-0.4109089	-0.0820164
C	3.8911324	0.5208269	0.9161973
C	-0.8085374	-0.7381248	2.8122022
C	-0.4617822	-0.3953618	4.1154096
C	0.5388020	0.5482459	3.9762209
C	-0.5162766	2.9143250	-0.5867584
C	-0.0828161	4.1545252	-0.1305472
C	0.8239432	3.8632266	0.8720797
C	0.1034414	-4.1468594	0.1272323
C	-0.8073552	-3.8620111	-0.8736507
C	-2.8679681	0.7414717	0.5561985
C	-4.1293066	0.3985514	0.0888722
C	-3.8942076	-0.5389658	-0.9034069
C	0.7963241	0.7458178	-2.8181104
C	0.4493061	0.3979446	-4.1199061
C	-0.5457338	-0.5508819	-3.9767030
H	-2.4306578	-2.2838169	-2.6543236
H	0.8629971	0.7828965	-5.0362847
H	-1.1153965	-1.0976049	-4.7107089
H	2.5732260	-1.4253815	-1.3393573
H	5.0743954	-0.7947625	-0.4122319
H	4.5725452	1.0518054	1.5613628
H	-1.5459629	-1.4385586	2.4534663
H	-0.8789265	-0.7804182	5.0301722
H	1.1103604	1.0898132	4.7125680
H	-1.2243420	2.6705517	-1.3624907
H	-0.3845227	5.1268362	-0.4808394
H	2.4308299	2.2788950	2.6583678
H	1.4139594	4.5075434	1.5037703
H	1.2338949	-2.6547289	1.3595921
H	0.4140576	-5.1170472	0.4755919
H	-1.3927517	-4.5105906	-1.5052704
H	-2.5795020	1.4365001	1.3284273
H	-5.0807482	0.7762834	0.4223898
H	-4.5748987	-1.0810295	-1.5400629
H	1.5306739	1.4510336	-2.4623941
N	-0.9008734	-2.5339792	-0.9911122
N	-0.0660507	-0.0390765	1.9562143
N	0.9055916	2.5346636	0.9919593
N	0.0911205	1.9500039	0.1024802
N	-0.0900436	-1.9437894	-0.1023269
N	-2.5771310	-0.7264337	-1.0037122
N	-1.9423000	0.0535382	-0.1140487
N	-0.7608468	-0.7401471	-2.6707451
N	0.0602371	0.0436995	-1.9590566
N	2.5753379	0.7216005	1.0073879
N	1.9390885	-0.0492917	0.1110019
N	0.7557427	0.7409248	2.6710298

---

Table ESI2: Optimised (unconstrained, ground-state) structure of  $[\text{Tp}_2\text{Fe}]^+$  with the counterion  $[\text{PF}_6]^-$ .

60			
Fe	-0.4985235	-0.1713451	-0.5516928
B	-1.9945025	-2.2559637	-2.2426733
B	1.0020995	1.8792647	1.1594530
C	0.3872507	-2.8963576	0.3799818
C	2.4095827	-0.6324731	-1.0276002
C	3.6140547	-0.1272827	-0.5694718
C	3.2674688	0.8945753	0.3069414
C	-1.2195063	-0.7177568	2.3063609
C	-0.8876026	-0.2296710	3.5626639
C	-0.0172625	0.8225406	3.3214579
C	-1.3873606	2.5655478	-1.4705460
C	-1.1204394	3.8937070	-1.1530917
C	-0.1960186	3.8289512	-0.1241727
C	0.1309523	-4.2334352	0.0822185
C	-0.7929483	-4.1957741	-0.9439812
C	-3.4457361	0.2401510	-0.0736465
C	-4.6499754	-0.3159451	-0.4894870
C	-4.2868932	-1.3278568	-1.3620286
C	0.2262107	0.3170036	-3.4412004
C	-0.0659582	-0.2207690	-4.6918312
C	-0.9372112	-1.2622077	-4.4308783
H	-2.5858903	-3.0622700	-2.9008804
H	0.3052812	0.1014349	-5.6496363
H	-1.4282746	-1.9589920	-5.0906975
H	2.2081221	-1.4384842	-1.7147007
H	4.6066971	-0.4636064	-0.8149154
H	3.8647876	1.5308427	0.9430570
H	-1.8610012	-1.5381615	2.0261545
H	-1.2114365	-0.6003523	4.5199356
H	0.5475274	1.4585640	3.9863660
H	-2.0483659	2.1487503	-2.2138745
H	-1.5385033	4.7759160	-1.6068286
H	1.5827675	2.6875787	1.8063286
H	0.3029329	4.6019439	0.4376817
H	1.0454370	-2.4617132	1.1165427
H	0.5592715	-5.1028907	0.5507469
H	-1.2812425	-4.9868810	-1.4895970
H	-3.2513303	1.0501681	0.6106414
H	-5.6447645	-0.0267515	-0.1965389
H	-4.8846249	-2.0266005	-1.9247282
H	0.8673170	1.1404848	-3.1700825
N	-1.0545570	-2.9135333	-1.2262829
N	-0.5970365	0.0038065	1.3724402
N	0.0517119	2.5440796	0.1367904
N	-0.6708071	1.7699206	-0.6789761
N	-0.3357065	-2.1202782	-0.4204132
N	-2.9545650	-1.3543910	-1.4450936
N	-2.4359200	-0.3977717	-0.6602425
N	-1.1337510	-1.3241219	-3.1097268
N	-0.4256630	-0.3620185	-2.5026778
N	1.9409551	0.9806240	0.3369404
N	1.4024653	0.0470874	-0.4683992
N	0.1261145	0.9438035	2.0021904
F	3.4246460	0.5806428	5.4105965
F	2.4452805	2.3854796	4.4073412
F	4.6350382	2.4927499	5.0630262
P	3.7879892	1.4973174	4.1472569
F	2.9055596	0.5069094	3.1902066
F	5.0899189	0.6145517	3.8336301
F	4.1059389	2.4212587	2.8396428

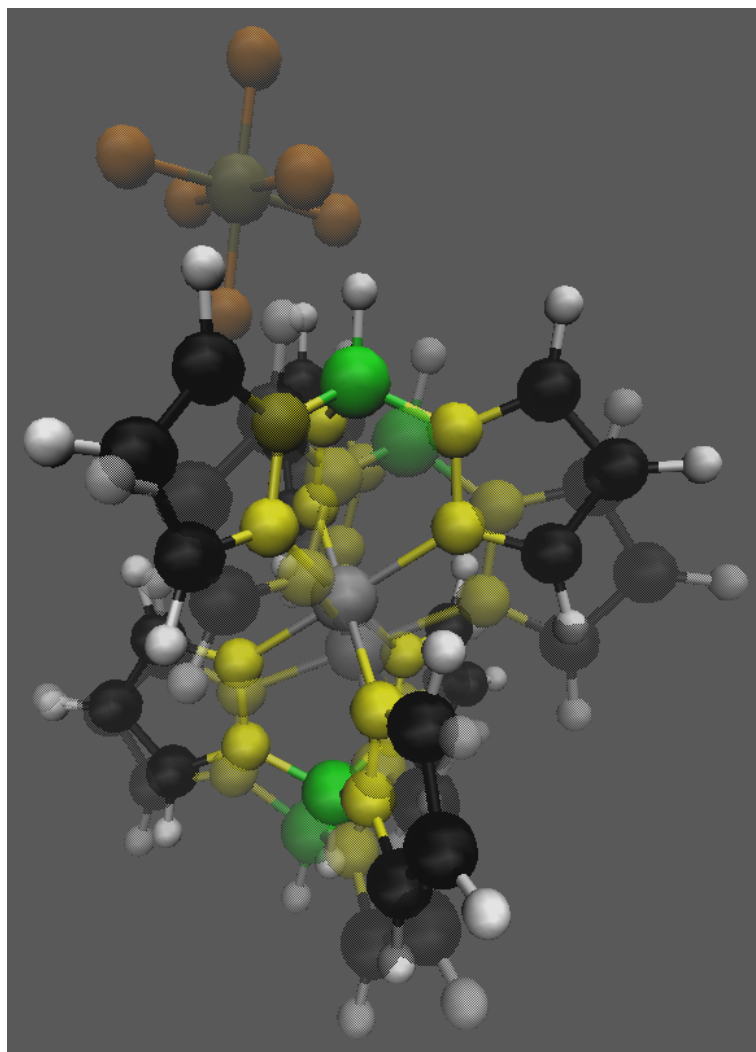


Figure ESI1: Optimised (unconstrained, ground-state) structure of  $[\text{Tp}_2\text{Fe}]^+$  *in vacuo* (opaque) and with the counterion  $[\text{PF}_6]^-$  (translucent). Fe atom in grey, N in yellow, B in green, C in black, H in white, P in tan and F in ochre.

Table ESI3: COSMO-optimised (unconstrained, ground-state) structure of  $[\text{Tp}_2\text{Fe}]^+$  in acetone ( $\epsilon = 20.7$ ).

---

53

---

Fe	-0.0000312	0.0001125	-0.0000586
B	-1.7537360	-1.6479291	-1.9017883
B	1.7540515	1.6469986	1.9023140
C	0.5366220	-2.9069798	0.5777300
C	2.8642136	-0.7531636	-0.5455665
C	4.1320863	-0.4211562	-0.0763849
C	3.9077489	0.5275629	0.9056105
C	-0.8146675	-0.7356487	2.7943081
C	-0.4623522	-0.3958094	4.0936413
C	0.5468867	0.5444300	3.9520107
C	-0.5354677	2.9075195	-0.5774231
C	-0.1125576	4.1519750	-0.1184856
C	0.8099121	3.8678069	0.8728130
C	0.1149553	-4.1517239	0.1184178
C	-0.8075555	-3.8681770	-0.8730172
C	-2.8643140	0.7539485	0.5442772
C	-4.1322070	0.4203538	0.0762857
C	-3.9077631	-0.5298170	-0.9042867
C	0.8129159	0.7367337	-2.7947620
C	0.4596542	0.3973412	-4.0939560
C	-0.5486266	-0.5438627	-3.9519030
H	-2.4312374	-2.2839118	-2.6523759
H	0.8761543	0.7801649	-5.0105188
H	-1.1213100	-1.0837099	-4.6893286
H	2.5724656	-1.4524277	-1.3131453
H	5.0785705	-0.8169531	-0.4046184
H	4.5921260	1.0638944	1.5435751
H	-1.5574904	-1.4317838	2.4380338
H	-0.8800482	-0.7777541	5.0100257
H	1.1193826	1.0841607	4.6896673
H	-1.2495584	2.6609789	-1.3470546
H	-0.4341869	5.1218891	-0.4591478
H	2.4316395	2.2826731	2.6530842
H	1.3916480	4.5167021	1.5080454
H	1.2502856	-2.6599797	1.3476056
H	0.4374419	-5.1214332	0.4588640
H	-1.3884702	-4.5174517	-1.5086149
H	-2.5726286	1.4546521	1.3105718
H	-5.0787757	0.8159996	0.4044457
H	-4.5921252	-1.0676722	-1.5409822
H	1.5555995	1.4331713	-2.4387857
N	-0.9148477	-2.5396440	-0.9766498
N	-0.0648669	-0.0434014	1.9355093
N	0.9160442	2.5391968	0.9767250
N	0.0976909	1.9493396	0.0943949
N	-0.0972595	-1.9492269	-0.0940227
N	-2.5899626	-0.7352544	-0.9939500
N	-1.9493550	0.0448006	-0.1121342
N	-0.7644118	-0.7361404	-2.6497918
N	0.0645075	0.0433709	-1.9356451
N	2.5900439	0.7338172	0.9948138
N	1.9493620	-0.0446167	0.1116354
N	0.7638043	0.7360349	2.6499925

---

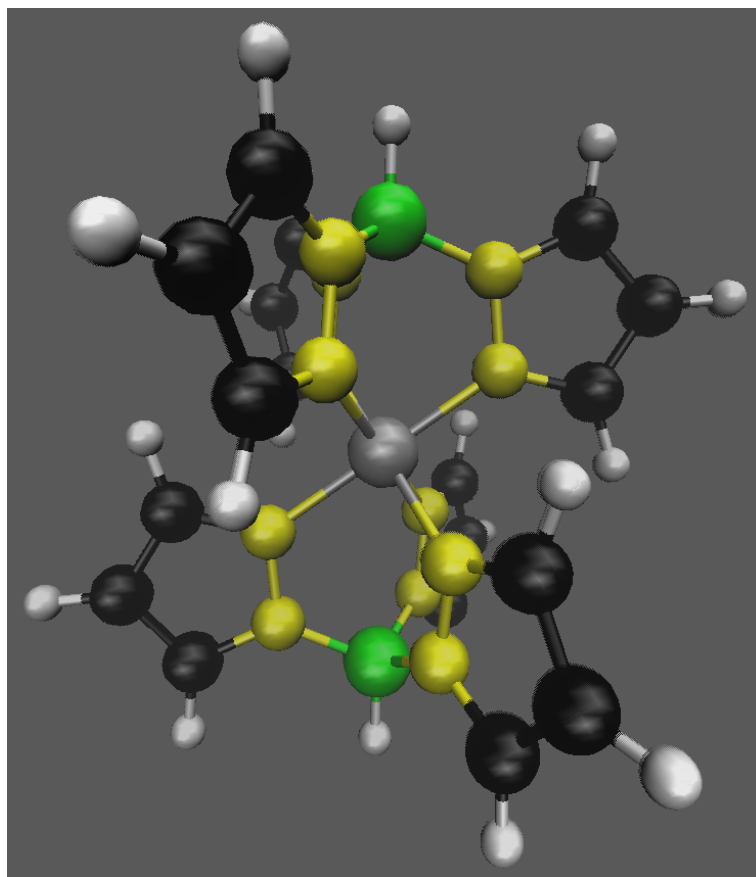


Figure ESI2: Optimised (unconstrained, ground-state) structure of  $[\text{Tp}_2\text{Fe}]^+$  *in vacuo* (opaque) and in acetone ( $\epsilon = 20.7$ ) using COSMO (translucent). The differences are very minor.

Table ESI4: Optimised (unconstrained, ground-state) structure of  $[\text{Tp}_2\text{Fe}]^+$  with 12 explicit acetone molecules. Optimised using the PBE functional.

173			
Fe	-0.4727024	-0.3190762	0.3666288
B	-2.6713957	-1.6929536	-1.3131827
B	1.7403693	1.0359065	2.0360824
C	-0.1359784	-3.2912263	0.7608219
C	2.1913472	-1.2097370	-0.7786306
C	3.5522276	-0.9623780	-0.5689122
C	3.5994453	-0.0927419	0.5188385
C	-0.8757719	-1.1797863	3.2390394
C	-0.2456815	-0.9897746	4.4772371
C	0.8277052	-0.1404612	4.2235469
C	-0.8218776	2.6654497	0.0284646
C	-0.2064544	3.8349688	0.4770615
C	0.8379587	3.4014931	1.2957186
C	-0.7368205	-4.4673655	0.3061663
C	-1.7667794	-4.0538669	-0.5418374
C	-3.1339064	0.6678775	1.4145023
C	-4.4907676	0.5033473	1.1080815
C	-4.5280667	-0.4033570	0.0516451
C	-0.0096793	0.4476780	-2.5499191
C	-0.5791539	0.1623303	-3.8007685
C	-1.6694988	-0.6637225	-3.5323576
H	-3.5262506	-2.2397300	-1.9576535
H	-0.2363188	0.5122414	-4.7682305
H	-2.3932571	-1.1479094	-4.1847805
H	1.7080643	-1.8234043	-1.5280929
H	4.3753245	-1.3757615	-1.1394248
H	4.4319835	0.4040939	1.0093197
H	-1.7570034	-1.7622212	2.9836520
H	-0.5409684	-1.4095593	5.4318728
H	1.5678436	0.3048023	4.8845358
H	-1.6828567	2.5333692	-0.6166990
H	-0.4877587	4.8496661	0.2196983
H	2.5976541	1.5791152	2.6798382
H	1.5902132	3.9498983	1.8542977
H	0.7153092	-3.1606664	1.4211625
H	-0.4563991	-5.4845488	0.5536518
H	-2.4563822	-4.6206357	-1.1594971
H	-2.6521288	1.2764745	2.1769684
H	-5.3347425	0.9724264	1.6003127
H	-5.3580071	-0.8566245	-0.4842334
H	0.8586771	1.0518566	-2.3022429
N	-1.7681971	-2.7077802	-0.5760594
N	-0.2079373	-0.4906453	2.2976380
N	0.8286751	2.0562377	1.3203231
N	-0.1866319	1.5938615	0.5433216
N	-0.7650528	-2.2321957	0.2143001
N	-3.2560558	-0.7455293	-0.2499252
N	-2.4005068	-0.0898214	0.5783870
N	-1.7332237	-0.8427778	-2.1957259
N	-0.7227660	-0.1674753	-1.5891039
N	2.3310285	0.1385735	0.9276425
N	1.4651085	-0.5390736	0.1323078
N	0.8307406	0.1432396	2.9008371
O	3.0426160	5.4751684	2.8334898
H	1.8669169	6.5287195	4.8229352
H	0.7301863	7.3207955	3.6840776
C	1.7909757	7.1823326	3.9474646
C	2.5278314	6.5875717	2.7727917
H	2.1829728	8.1826434	4.1861893
C	2.5925319	7.4176685	1.5142946
H	1.5834611	7.7298019	1.2041457
H	3.0758603	6.8561467	0.7076281
H	3.1565913	8.3437177	1.7083544
O	-3.6545298	-2.3322349	-5.7292946
H	-5.1597667	-2.9784964	-7.6652988
H	-3.7347221	-3.5100497	-8.6272829
C	-4.1708914	-2.6893143	-8.0367392
C	-3.2600707	-2.3207650	-6.8892966
H	-4.2721203	-1.8358521	-8.7255408
C	-1.8413496	-1.9413722	-7.2449715
H	-1.3636334	-2.7534719	-7.8142911
H	-1.2558280	-1.7312749	-6.3435573
H	-1.8406983	-1.0597019	-7.9045882
C	-1.8969787	1.9324946	5.8402947
H	-1.1522603	1.5365959	6.5459532
C	-1.2233912	2.7003686	4.7270387
O	-1.5193259	2.5286296	3.5521897
H	0.1366730	4.3032505	4.2774219
C	-0.1634712	3.6943399	5.1374096
H	0.7139183	3.1507705	5.5275647
H	-0.5248590	4.3366854	5.9550610
H	-2.5432827	2.6179571	6.4121662
H	-2.5023905	1.1167719	5.4311209
C	3.5714344	2.8699434	-1.6708511
O	2.4845251	2.4723719	-2.0720517
H	4.4759351	4.7639930	-1.1534170
C	3.6896461	4.0868677	-0.7862958
H	2.7283456	4.6080155	-0.7248354
H	3.9996740	3.7598929	0.2197102
H	5.4625200	2.8204228	-2.6751820
C	4.8566614	2.1650597	-2.0287972
H	4.6456293	1.2268734	-2.5522697
H	5.4503662	1.9736713	-1.1223030
H	4.6863866	-2.8040914	4.0212240
C	3.9410665	-2.3993789	3.3184941
H	2.9629907	-2.3271934	3.8072042
H	4.2883589	-1.3944905	3.0329968

C	3.8581026	-3.2725827	2.0876210
O	2.8007154	-3.7766897	1.7333167
H	5.7160835	-4.2978635	1.8614473
C	5.1425747	-3.5187762	1.3321816
H	4.9297378	-3.8647972	0.3140924
H	5.7724069	-2.6189894	1.3053373
H	2.4743052	-5.1729444	-0.2457137
C	2.6404702	-5.5885420	-1.2550168
H	3.6390520	-6.0433312	-1.2635172
H	1.8699792	-6.3455601	-1.4497849
O	3.5648725	-3.7206942	-2.4219151
C	2.5902253	-4.4372616	-2.2324726
H	1.3208214	-3.2922384	-3.5538349
C	1.2701605	-4.1893134	-2.9254197
H	0.9981862	-5.0604944	-3.5418455
H	0.4620275	-4.0959502	-2.1830056
O	-3.7739151	-2.6516326	2.7045408
C	-4.8375234	-3.0260563	2.2302206
C	-4.9087208	-4.1482620	1.2207179
H	-3.9354253	-4.6421314	1.1315551
H	-5.2093572	-3.7287146	0.2469094
H	-5.6854088	-4.8759331	1.4995084
H	-6.7471875	-2.1618301	1.7197002
C	-6.1538917	-2.3936355	2.6172605
H	-5.9829144	-1.4914512	3.2139222
H	-6.7412156	-3.1156595	3.2076379
O	-1.6499198	5.4499883	-1.8977525
C	-1.2665240	4.7050613	-2.7886831
H	0.7181903	3.9136354	-2.7876348
C	0.1596556	4.7264138	-3.2849302
H	0.6341774	5.6806385	-3.0268600
H	0.2226435	4.5465622	-4.3675913
H	-3.1539108	3.6706037	-2.9043079
C	-2.1894999	3.6882826	-3.4243929
H	-2.3510353	3.9490225	-4.4826460
H	-1.7293915	2.6872554	-3.4166416
H	5.0839832	4.0284018	5.9480567
C	4.0238694	3.8384599	5.7301770
H	5.6968060	1.5107665	5.6066445
H	3.3882039	4.2860913	6.5031563
H	3.7889097	4.3230234	4.7653972
C	4.7934706	1.5001214	4.9765735
C	3.7243352	2.3659965	5.6001978
H	5.0775574	1.9037168	3.9929572
O	2.6484170	1.8992591	5.9540181
H	4.4371920	0.4703784	4.8635064
H	6.8599384	4.7211702	3.2653172
C	6.4016276	4.4787042	2.2949513
H	8.1786384	2.4031951	3.2692897
H	5.3321265	4.7188302	2.3037841
H	6.9080945	5.1129584	1.5483573
C	8.0086461	2.4714460	2.1824523
C	6.6295371	3.0310962	1.9321502
H	8.7850114	3.1450975	1.7902740
O	5.7337865	2.3409905	1.4572521
H	8.1086080	1.4752696	1.7380321
H	-4.7138231	-4.3690413	-4.7810659
H	-2.8934586	-5.2650629	-6.5367087
C	-4.4563358	-5.3420325	-4.3307100
H	-4.8180305	-5.3719502	-3.2967541
C	-2.3358385	-5.7546455	-5.7266118
C	-2.9546220	-5.4837367	-4.3716947
H	-4.9473332	-6.1204835	-4.9335695
H	-2.3788014	-6.8395349	-5.9174127
H	-1.2844202	-5.4450029	-5.7337811
O	-2.2645895	-5.3883670	-3.3671100
H	-9.6545203	-2.3872047	-2.6859721
H	-7.4043773	-1.7526032	-3.9699664
C	-9.0721594	-2.9665791	-1.9541297
H	-9.4754725	-2.8184899	-0.9466470
C	-6.9569587	-2.5549711	-3.3618434
C	-7.6132647	-2.5802281	-2.0012136
H	-9.1808899	-4.0257370	-2.2377486
H	-7.1483740	-3.4947586	-3.9015519
H	-5.8785580	-2.3835538	-3.2744739
O	-6.9926799	-2.3010738	-0.9825648



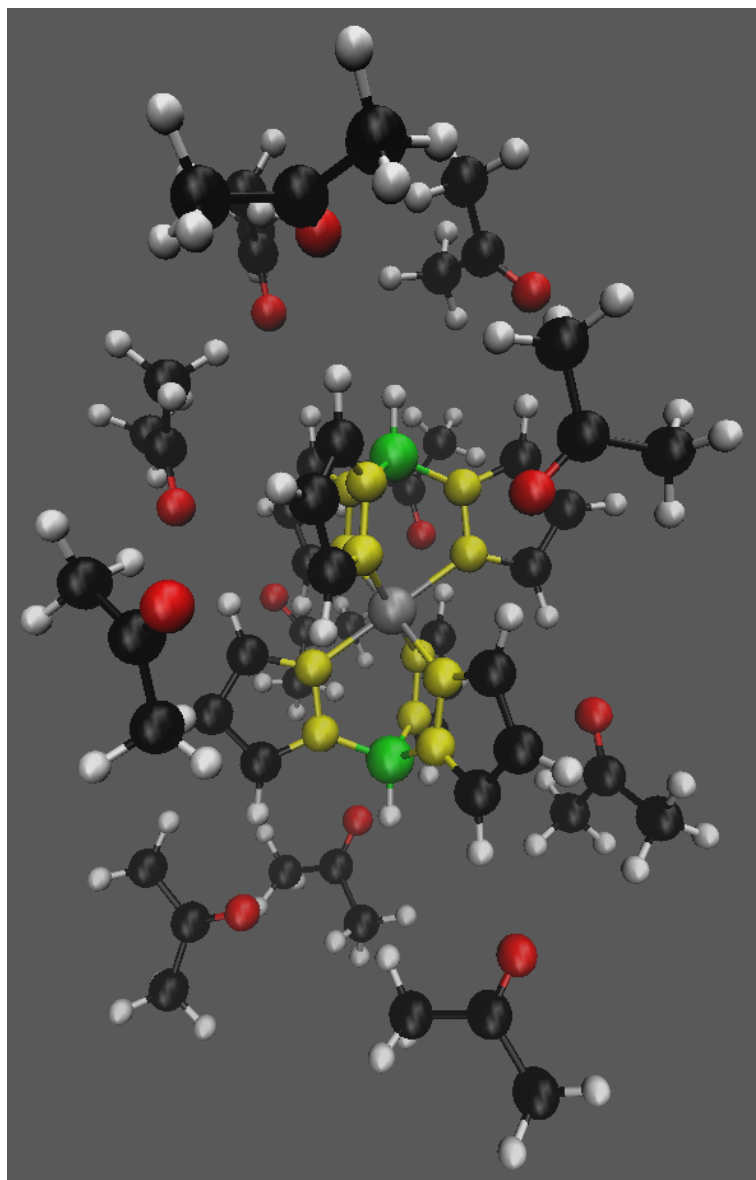


Figure ESI3: Optimised (unconstrained, ground-state) structure of  $[\text{Tp}_2\text{Fe}]^+$  with 12 acetone solvent molecules.

Table ESI5: Optimised structure of  $\text{Tp}_2\text{Fe}$  ( $S = 2$ ).

53			
Fe	-0.0012171	0.0012387	0.0000880
B	-1.8135685	-1.7033713	-1.9851814
B	1.8122607	1.7040380	1.9858595
C	0.4001434	-3.1893783	0.4487060
C	3.1548519	-0.6408543	-0.4137649
C	4.3779665	-0.2366638	0.1243970
C	4.0339206	0.6892143	1.0903187
C	-0.7066562	-0.6270299	3.1086745
C	-0.2789539	-0.2246520	4.3755757
C	0.7153919	0.6995427	4.1198472
C	-0.3903369	3.1922111	-0.4568441
C	0.1041621	4.3880666	0.0675638
C	0.9894498	3.9872434	1.0495057
C	-0.0888630	-4.3858309	-0.0794798
C	-0.9786044	-3.9859733	-1.0577930
C	-3.1583873	0.6333442	0.4211664
C	-4.3814506	0.2242783	-0.1133922
C	-4.0364509	-0.6987316	-1.0817028
C	0.6990022	0.6341763	-3.1088301
C	0.2704520	0.2322735	-4.3755920
C	-0.7221013	-0.6937557	-4.1195335
H	-2.5012341	-2.3458566	-2.7338781
H	0.6276179	0.5645563	-5.3358445
H	-1.3425721	-1.2716071	-4.7855962
H	2.9439852	-1.3530714	-1.1971015
H	5.3664509	-0.5672534	-0.1470127
H	4.6419762	1.2694977	1.7656122
H	-1.4688870	-1.3384839	2.8286762
H	-0.6377029	-0.5555695	5.3357122
H	1.3360140	1.2769750	4.7861321
H	-1.1082074	3.0264220	-1.2458029
H	-0.1437437	5.3952978	-0.2224830
H	2.5002734	2.3459011	2.7347711
H	1.6099822	4.5579745	1.7215645
H	1.1190176	-3.0227907	1.2365832
H	0.1652192	-5.3928327	0.2059890
H	-1.5973769	-4.5574102	-1.7308707
H	-2.9481816	1.3453447	1.2048774
H	-5.3704948	0.5501157	0.1616922
H	-4.6441380	-1.2809449	-1.7556655
H	1.4603881	1.3466386	-2.8291087
N	-0.9953853	-2.6465911	-1.0872328
N	-0.0211512	0.0091447	2.1671357
N	0.9986243	2.6479148	1.0845171
N	0.1565480	2.1552724	0.1646539
N	-0.1540284	-2.1530130	-0.1672571
N	-2.7015427	-0.8103137	-1.0994227
N	-2.1585800	0.0025681	-0.1816475
N	-0.8509674	-0.8144733	-2.7914337
N	0.0156406	-0.0039588	-2.1670499
N	2.6995012	0.8069944	1.1032868
N	2.1559258	-0.0046818	0.1848295
N	0.8460179	0.8188482	2.7917862

Table ESI6: Optimised structure of  $\text{Tp}_2\text{Fe}$  ( $S = 0$ ).

---

53

---

Fe	-0.0001357	0.0001799	-0.0000244
B	-1.7485489	-1.6398187	-1.9098848
B	1.7487464	1.6394187	1.9100577
C	0.5062275	-2.9476693	0.5662382
C	2.9069256	-0.7294071	-0.5342239
C	4.1728255	-0.3814197	-0.0551463
C	3.9241255	0.5538851	0.9290180
C	-0.7988885	-0.7175765	2.8498197
C	-0.4332725	-0.3685421	4.1527805
C	0.5715316	0.5639058	3.9909620
C	-0.5056940	2.9482184	-0.5659317
C	-0.0697273	4.1890310	-0.0935058
C	0.8368513	3.8806316	0.9006758
C	0.0708701	-4.1886837	0.0937784
C	-0.8357879	-3.8806966	-0.9004620
C	-2.9073324	0.7295374	0.5336342
C	-4.1731491	0.3808097	0.0548731
C	-3.9241917	-0.5548308	-0.9289042
C	0.7977406	0.7185161	-2.8499946
C	0.4324191	0.3689626	-4.1529000
C	-0.5715979	-0.5643055	-3.9909309
H	-2.4338460	-2.2825682	-2.6581797
H	0.8405983	0.7421092	-5.0769657
H	-1.1560562	-1.1133387	-4.7112815
H	2.6257154	-1.4267437	-1.3073549
H	5.1288007	-0.7568967	-0.3789830
H	4.5906973	1.1028579	1.5742235
H	-1.5456974	-1.4139227	2.5023400
H	-0.8416898	-0.7415706	5.0767883
H	1.1563894	1.1123954	4.7114020
H	-1.2157005	2.7125212	-1.3426286
H	-0.3716409	5.1672530	-0.4277017
H	2.4341863	2.2819214	2.6584321
H	1.4277221	4.5105044	1.5457085
H	1.2160884	-2.7116635	1.3429714
H	0.3732014	-5.1667673	0.4280008
H	-1.4263081	-4.5108328	-1.5455612
H	-2.6263004	1.4274193	1.3063409
H	-5.1292421	0.7559905	0.3787082
H	-4.5906168	-1.1042743	-1.5738579
H	1.5439313	1.4155818	-2.5026287
N	-0.9151115	-2.5456833	-0.9921074
N	-0.0640942	-0.0416269	1.9754194
N	0.9155467	2.5455786	0.9923656
N	0.0978680	1.9715554	0.0993735
N	-0.0977719	-1.9712823	-0.0990801
N	-2.5978065	-0.7314504	-1.0091533
N	-1.9723175	0.0499769	-0.1182042
N	-0.7696492	-0.7388321	-2.6766978
N	0.0636878	0.0419068	-1.9754832
N	2.5978035	0.7309773	1.0091914
N	1.9720972	-0.0498798	0.1179181
N	0.7695776	0.7386379	2.6767562

---

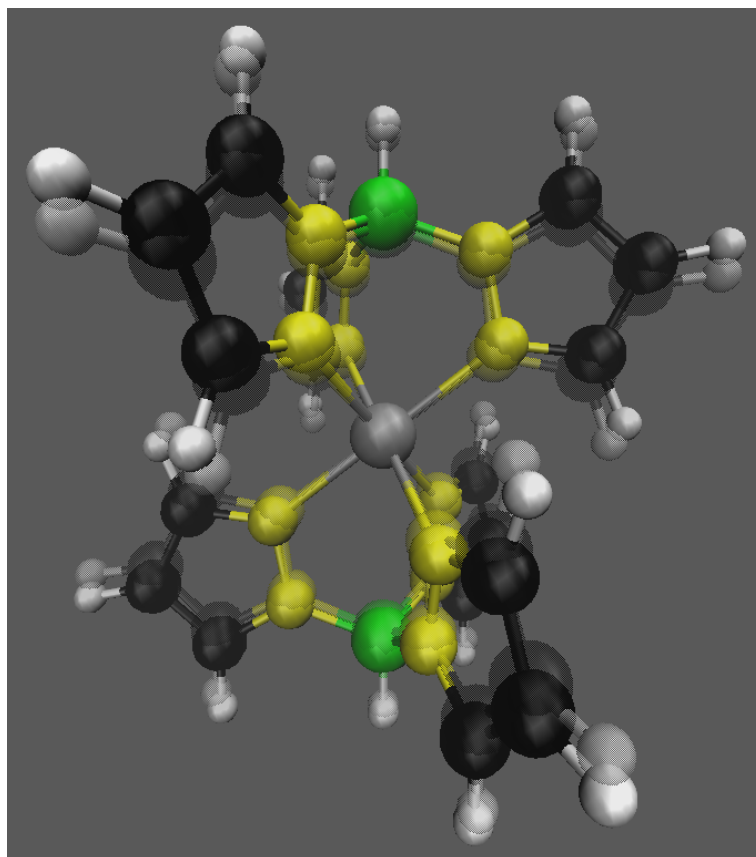


Figure ESI4: Optimised structure of  $\text{Tp}_2\text{Fe}$  in the  $S = 2$  state (opaque) and the  $S = 0$  state (translucent).

## Reference shieldings

Table ESI7: Computed NMR reference shieldings (ppm).

Nucleus [reference]	PBE	PBE-25	PBE-40	PBE-100
H [TMS]	31.7	31.8	31.8	31.2
C [TMS]	184.6	188.4	190.4	182.7
B [BF <sub>3</sub> (O(C <sub>2</sub> H <sub>5</sub> ) <sub>2</sub> )]	96.5	101.9	105.0	91.1
N [CH <sub>3</sub> NO <sub>2</sub> ]	-114.0	-139.3	-154.7	-63.1

## Zero-field splitting parameters

The zero-field splitting  $D$ -parameter is defined as

$$D = D_{33} - \frac{1}{2}(D_{11} + D_{22}), \quad (1)$$

where  $D_{11}$ ,  $D_{22}$  and  $D_{33}$  are the eigenvalues of the traceless zero-field splitting tensor. The  $E$ -parameter is

$$E = \frac{1}{2}(D_{11} - D_{22}). \quad (2)$$

The eigenvalues  $D_{11}$ ,  $D_{22}$  and  $D_{33}$  are conventionally assigned so that the condition  $E/D > 0$  is satisfied.

## Full numerical pNMR results for $[\text{Tp}_2\text{Fe}]^+$

Table ESI8: Experimental and computational NMR chemical shifts (ppm) for  $[\text{Tp}_2\text{Fe}]^+$ . Functional PBE-25 was used unless indicated otherwise. The  $g$ -tensor was calculated at the NEVPT2 level based on the indicated CASSCF wavefunction. Geometry optimised *in vacuo* was used in  $g$ -tensor calculations. In counterion and explicit solvent HFC calculations, the corresponding geometry was used; otherwise *in vacuo* unless otherwise indicated. Temperature for  $^1\text{H}$ : 305 K;  $^{13}\text{C}$ : 300 K;  $^{11}\text{B}$  and  $^{14}\text{N}$ : 298 K.

Wavefunction, HFC level	H3	H4	H5	BH	C3	C4	C5	B	N1	N2
exptl <sup>2,3</sup>	-52.9	-13.2	-8.2	39.4	2.5	175.8	19.6	95.2	-	-
cas(5,5), mDKS	-51.3	-10.0	-2.0	41.5	34.7	-3.6	93.7	91.2	-419.5	-2940.1
cas(9,12), mDKS (PBE)	-44.1	-19.2	-0.5	37.6	-21.8	-3.3	58.9	71.1	-370.0	-1918.5
cas(9,12), mDKS (PBE-25)	-50.9	-9.4	0.3	42.0	34.6	2.5	91.6	92.5	-396.8	-2758.0
cas(9,12), mDKS (PBE-40)	-55.2	-5.5	-0.6	44.1	76.6	-0.1	108.9	104.3	-423.9	-3165.0
cas(9,12), mDKS (PBE-100)	-63.3	17.2	-15.6	38.3	312.9	-64.1	235.5	115.2	-474.8	-3079.4
cas(9,12), DKH	-43.9	-9.1	-2.6	36.6	61.2	2.9	88.5	78.5	-412.9	-2875.8
cas(9,12), DKH + $[\text{PF}_6]^-$	-41.9	-11.5	-3.7	34.4	58.2	8.5	96.4	74.1	-414.5	-2739.0
cas(9,12), DKH + C-PCM	-44.3 <sup>a</sup>	-8.9 <sup>a</sup>	-2.5 <sup>a</sup>	36.6 <sup>a</sup>	61.7 <sup>b</sup>	4.3 <sup>b</sup>	89.9 <sup>b</sup>	78.9 <sup>c</sup>	-	-
cas(9,12), DKH + C-PCM <sup>a</sup>					60.3	2.5	89.0	78.9	-411.7	-2877.8
cas(9,12), DKH + C-PCM <sup>a,d</sup>	-43.8	-9.3	-2.3	36.4	70.3	3.8	102.3	78.5	-415.7	-2857.1
cas(9,12), DKH + 12 acetones	-41.8	-7.9	-4.7	34.6	68.1	-2.0	106.0	75.1	-429.8	-2907.7
cas(9,12), DLPNO-CCSD	-44.5	-2.4	6.5	37.6	73.9	16.3	136.2	76.1	-260.5	-3039.6

<sup>a</sup> Acetone-d<sub>6</sub> ( $\epsilon = 20.7$ ).

<sup>b</sup> Chloroform ( $\epsilon = 4.81$ ).

<sup>c</sup> Dichloromethane ( $\epsilon = 8.93$ ).

<sup>d</sup> COSMO-optimised geometry used in the HFC calculation.

## Temperature series of $[\text{Tp}_2\text{Fe}]^+$

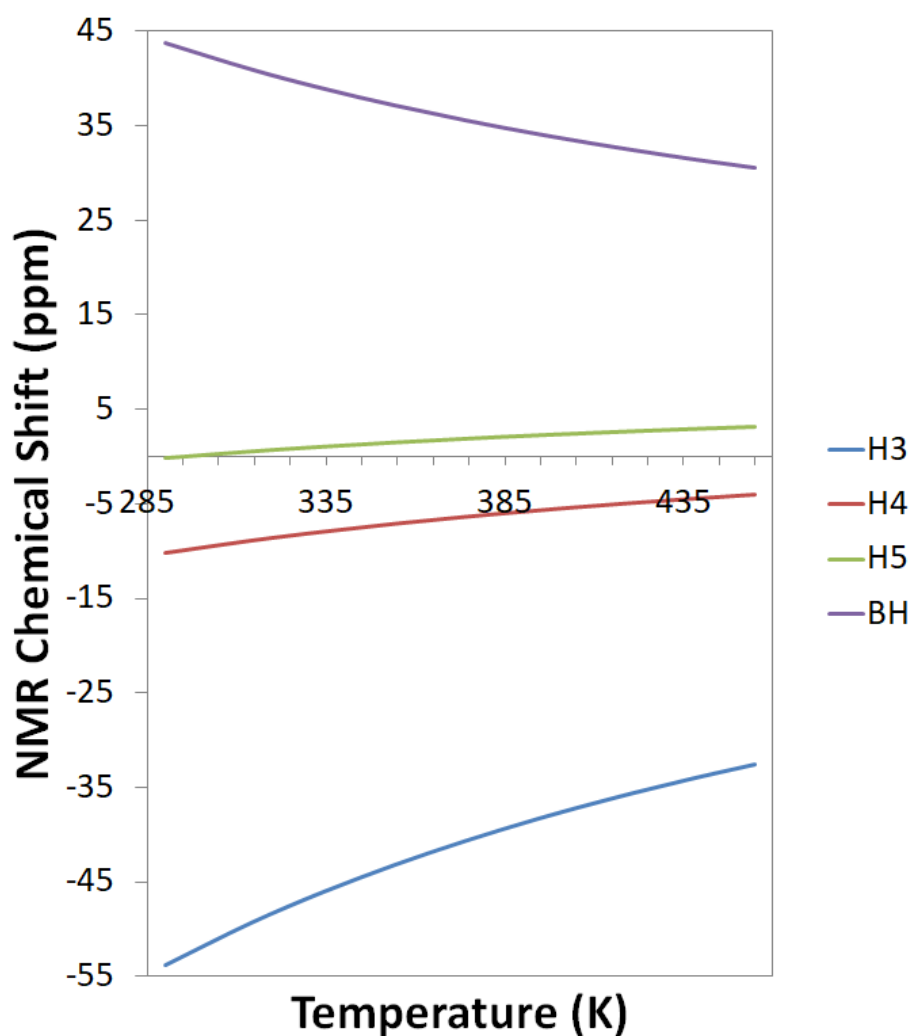


Figure ESI5: Computational  $^1\text{H}$  temperature series of  $[\text{Tp}_2\text{Fe}]^+$  calculated at the mDKS/PBE0 level of theory for HFCs and cas(9,12)/NEVPT2 level for the  $g$ -tensor. Contribution from the ground-state doublet only.

## Excited state of $[\text{Tp}_2\text{Fe}]^+$

The thermal Boltzmann equilibrium of the ground state and a doublet excited state of  $[\text{Tp}_2\text{Fe}]^+$  was fitted to experimental signal shifts similarly to the case of the spin-crossover complex  $\text{Tp}_2\text{Fe}$ , with  $\Delta E$  and  $\Delta S$  between the ground and excited states acting as fitting parameters. The  $g$ -tensor and the HFCs of the excited state were estimated using the ORCA programme in order to determine the nuclear shieldings in the excited doublet. The orbital shieldings were approximated to be the same as for the ground state. This is a severe approximation, dictated by our present lack of means to directly compute the orbital shielding tensor for the excited state.

Due to the need to adjust orbital occupations to create a configuration corresponding to the electronically excited multiplet, the excited-state calculations were performed with a symmetry-optimised geometry in the  $D_{3d}$  point group. The TURBOMOLE programme was used at the standard level of theory for the constrained geometry optimisation. Due to the orbital degeneracy of the  $D_{3d}$  electronic structure in the ground configuration,  $\dots 2a_{2g}^2 3a_{1u}^2 3a_{2g}^2 19e_g^3$ , an initial Fermi smearing step was performed before the geometry optimisation. The resulting  $D_{3d}$  structure is provided in Table ESI9.

Table ESI9: Optimised structure of  $[\text{Tp}_2\text{Fe}]^+$  in  $D_{3d}$  symmetry.

53			
Fe	0.0000000	-0.0000000	0.0000000
B	0.0000000	0.0000000	-3.0601708
B	0.0000000	-0.0000000	3.0601708
C	-2.4879087	1.4363947	-0.8778219
C	-2.4879087	-1.4363947	0.8778219
C	-3.1091790	-1.7950853	2.0677482
C	-2.2733922	-1.3125436	3.0612238
C	-0.0000000	2.8727895	0.8778219
C	0.0000000	3.5901707	2.0677482
C	-0.0000000	2.6250872	3.0612238
C	2.4879087	-1.4363947	0.8778219
C	3.1091790	-1.7950853	2.0677482
C	2.2733922	-1.3125436	3.0612238
C	-3.1091790	1.7950853	-2.0677482
C	-2.2733922	1.3125436	-3.0612238
C	2.4879087	1.4363947	-0.8778219
C	3.1091790	1.7950853	-2.0677482
C	2.2733922	1.3125436	-3.0612238
C	-0.0000000	-2.8727895	-0.8778219
C	0.0000000	-3.5901707	-2.0677482
C	0.0000000	-2.6250872	-3.0612238
H	0.0000000	0.0000000	-4.2553543
H	-0.0000000	-4.6596441	-2.1923746
H	0.0000000	-2.7155395	-4.1357668
H	-2.7907466	-1.6112383	-0.1420277
H	-4.0353701	-2.3298220	2.1923746
H	-2.3517262	-1.3577697	4.1357668
H	0.0000000	3.2224766	-0.1420277
H	0.0000000	4.6596441	2.1923746
H	0.0000000	2.7155395	4.1357668
H	2.7907466	-1.6112383	-0.1420277
H	4.0353701	-2.3298220	2.1923746
H	0.0000000	-0.0000000	4.2553543
H	2.3517262	-1.3577697	4.1357668
H	-2.7907466	1.6112383	0.1420277
H	-4.0353701	2.3298220	-2.1923746
H	-2.3517262	1.3577697	-4.1357668
H	2.7907466	1.6112383	0.1420277
H	4.0353701	2.3298220	-2.1923746
H	2.3517262	1.3577697	-4.1357668
H	0.0000000	-3.2224766	0.1420277
N	-1.2318313	0.7111981	-2.4787227
N	0.0000000	1.5658372	1.1436949
N	1.2318313	-0.7111981	2.4787227
N	1.3560548	-0.7829186	1.1436949
N	-1.3560548	0.7829186	-1.1436949
N	1.2318313	0.7111981	-2.4787227
N	1.3560548	0.7829186	-1.1436949
N	0.0000000	-1.4223963	-2.4787227
N	0.0000000	-1.5658372	-1.1436949
N	-1.2318313	-0.7111981	2.4787227
N	-1.3560548	-0.7829186	1.1436949
N	0.0000000	1.4223963	2.4787227

The  $g$ -tensor of the excited doublet was calculated using the pseudospin formalism discussed, *e.g.*, by Chibotaru *et al.*<sup>4</sup> at the NEVPT2 level based on a  $\text{cas}(5,5)$  wavefunction, using the SINGLE\_ANISO module of ORCA and requesting the  $g$ -tensors of the two lowest doublet multiplets. The resulting  $g$ -tensor eigenvalues for the excited doublet were  $|g_i| = 0.63, 0.24$  and  $0.24$ , with a negative sign indicated for the product  $g_1 g_2 g_3$ . Due to the  $D_{3d}$  symmetry of the complex, it is reasonable to assume a cylindri-



cally symmetric  $g$ -tensor, meaning that  $g_1 = -0.63$  along the 3-fold molecular axis and  $g_2 = g_3 = 0.24$  in the two perpendicular directions. The approximate  $g$ -tensor for the excited doublet is thereby fixed.

As for the HFCs, an initial DFT calculation was performed at the DKH2/PBE0 level, using the optimised  $D_{3d}$  geometry, for the ground electron configuration. Low-lying excited, orbitally non-degenerate configurations can be obtained from the ground configuration by exchanging occupied and unoccupied  $\beta$ -spin orbitals to  $\dots 2a_{2g}^2 3a_{1u}^2 3a_{2g}^1 19e_g^4, \dots 2a_{2g}^2 3a_{1u}^1 3a_{2g}^2 19e_g^4$  and  $\dots 2a_{2g}^1 3a_{1u}^2 3a_{2g}^2 19e_g^4$ , in an order based on differences in the exchanged orbital energies. The first of these configurations is expected to correspond to the lowest excited doublet and, hence, the expectation-value (the contact and dipolar) contributions to the HFCs were then computed for it. The orbital contributions had to be omitted from the HFC, due to the fact that they would have required wave function response, which was not available for the present excited-state case. Due to the many approximations, it is clear that the result is only an estimate for the true excited-state HFCs. In the Boltzmann fitting process, all possible assignments of the three carbon signals were considered separately. In addition, the thermal average was calculated with  $\Delta E$  fixed to 6.4 kJ/mol, as determined computationally at the cas(9,12)/NEVPT2 level of theory, and  $\Delta S$  fixed to zero. Because the part of the entropy coming from the degeneracy  $2S + 1 = 2$  of the electronic states is the same for both lowest doublets, the latter approximation entails that also the vibrational entropy is assumed to be the same for both doublets. A further underlying approximation in the present Boltzmann averaging is that the magnetic coupling terms<sup>5</sup> between the ground- and excited-doublet states are not accounted for. The results are shown in Table ESI10.

Table ESI10: Ground-state and approximate excited-state nuclear shieldings for  $[\text{Tp}_2\text{Fe}]^+$ , along with the chemical shifts of fitted Boltzmann averages (ppm) with different assignments of the carbon signals. The  $g$ -tensor for the ground state has been calculated at the NEVPT2 level based on a cas(9,12) wavefunction, and for the excited state at the cas(5,5)/NEVPT2 level using the pseudospin formalism. The HFCs were computed at the DKH2/PBE0 level. The Boltzmann averages have also been calculated with  $\Delta E = 6.4$  kJ/mol computed at the cas(9,12)/NEVPT2 level with  $\Delta S$  set to zero, and the experimental and pure ground-state chemical shifts have been included for comparison. The fitting parameters  $\Delta E$  (kJ/mol) and  $\Delta S$  (J/Kmol) are reported for the fitted shifts.

	H3	H4	H5	BH	C3	C4	C5	B	N1	N2	$\Delta E$	$\Delta S$
Nuclear shieldings												
ground state	75.7	40.9	34.4	-4.8	127.2	185.5	99.9	23.4	273.6	2736.5		
excited state	25.6	29.9	19.4	22.5	70.4	114.1	43.9	105.3	74.1	-69.7		
Boltzmann-average shifts												
exptl	-52.9	-13.2	-8.2	39.4	2.5	175.8	19.6	95.2	-	-		
pure ground state	-43.9	-9.1	-2.6	36.6	61.2	2.9	88.5	78.5	-412.9	-2875.8		
assignment 345	-37.4	-7.7	-0.7	33.1	69.5	13.2	96.6	66.0	-382.6	-2448.7	-20.4	-82.7
assignment 534	-42.9	-8.9	-2.3	36.1	62.5	4.4	89.7	76.6	-408.3	-2810.8	-17.3	-89.2
assignment 354	-42.4	-8.7	-2.2	35.8	63.1	5.3	90.4	75.6	-405.9	-2776.8	-17.5	-86.3
assignment 435	-42.6	-8.8	-2.3	35.9	62.8	4.8	90.0	76.1	-407.1	-2794.1	-17.4	-87.5
assignment 453	-42.1	-8.7	-2.1	35.6	63.5	5.7	90.7	75.0	-404.6	-2758.3	-17.6	-85.2
assignment 543	-37.4	-7.7	-0.7	33.0	69.5	13.3	96.7	65.9	-382.4	-2446.8	-20.4	-82.7
$\Delta E$ comptl, $\Delta S$ zero	-40.2	-8.3	-1.5	34.6	65.2	7.9	92.4	72.8	-399.2	-2682.0	6.4	0

Including the doublet excited state in a thermal equilibrium does not improve the agreement with experiment regardless of which carbon signal assignment is used in the fit, nor when a computational value for  $\Delta E$  is used. Furthermore, the fit in each case incorrectly places the excited doublet below the ground doublet in energy. A probable cause is a failure of the employed approximations to reasonably estimate the excited-state EPR parameters. Considering the sensitivity of the nuclear shieldings to the HFCs, the present method of approximating the excited-state electronic structure used in their calculation is likely to be inadequate. More work in this direction will be needed in the future.

# Physical contributions to the isotropic nuclear shieldings

The HFC tensor can be decomposed as

$$\mathbf{A} = A_{\text{con}}\mathbf{1} + \mathbf{A}_{\text{dip}} + A_{\text{pc}}\mathbf{1} + \mathbf{A}_{\text{dip},2} + \mathbf{A}_{\text{as}}, \quad (3)$$

where  $A_{\text{con}}$  and  $\mathbf{A}_{\text{dip}}$  are the nonrelativistic isotropic contact coupling and anisotropic dipolar coupling tensors, respectively. The rest of the tensors are relativistic in their origin:  $A_{\text{pc}}$  is the isotropic pseudo-contact coupling,  $\mathbf{A}_{\text{dip},2}$  is the anisotropic and symmetric second dipolar term,  $\mathbf{A}_{\text{as}}$  is the antisymmetric term and  $\mathbf{1}$  is a unit tensor. The  $g$ -tensor can similarly be decomposed as

$$\mathbf{g} = g_e\mathbf{1} + \Delta g_{\text{iso}}\mathbf{1} + \Delta\tilde{\mathbf{g}}, \quad (4)$$

where  $g_e$  is the free-electron  $g$ -factor, and  $\Delta g_{\text{iso}}$  and  $\Delta\tilde{\mathbf{g}}$  are the isotropic and anisotropic parts of the  $g$ -shift tensor. The isotropic nuclear shielding constant  $\sigma$  can be broken down to its physical contributions by the decompositions of the HFC tensor and the  $g$ -tensor. These contributions are, up to order  $\mathcal{O}(\alpha^4)$  in the fine structure constant  $\alpha$ ,

$$\sigma = \sigma_{\text{orb}} + \sigma_{\text{con}} + \sigma_{\text{con},2} + \sigma_{\text{con},3} + \sigma_{\text{dip}} + \sigma_{\text{dip},2} + \sigma_{\text{dip},3} + \sigma_{\text{c,aniso}} + \sigma_{\text{pc}}, \quad (5)$$

where  $\sigma_{\text{orb}}$  is the orbital shielding term. See Table ESI11 for a detailed breakdown of the other contributions.

Table ESI11: Classification of nuclear shielding terms in doublet and higher-multiplicity spin states. Terms 3 and 4 are not extracted separately from terms 1 and 2, respectively, when the HFC tensors are obtained from a fully relativistic mDKS calculation. Term 5 does not contribute to the isotropic shielding.

Term in $\sigma_{\epsilon\tau}$	Number	Symbol	Order	Tensorial rank <sup>a</sup>	
				$S = 1/2$	$S > 1/2$
$g_e A_{\text{con}} \langle S_\epsilon S_\tau \rangle$	1	$\sigma_{\text{con}}$	$\mathcal{O}(\alpha^2)$	0	0, 2
$g_e \sum_b A_{b\tau}^{\text{dip}} \langle S_\epsilon S_b \rangle$	2	$\sigma_{\text{dip}}$	$\mathcal{O}(\alpha^2)$	2	0, 2, 1
$g_e A_{\text{pc}} \langle S_\epsilon S_\tau \rangle$	3	$\sigma_{\text{con},2}$	$\mathcal{O}(\alpha^4)$	0	0, 2
$g_e \sum_b A_{b\tau}^{\text{dip},2} \langle S_\epsilon S_b \rangle$	4	$\sigma_{\text{dip},2}$	$\mathcal{O}(\alpha^4)$	2	0, 2, 1
$g_e \sum_b A_{b\tau}^{\text{as}} \langle S_\epsilon S_b \rangle$	5	$\sigma_{\text{as}}$	$\mathcal{O}(\alpha^4)$	1	2, 1
$\Delta g_{\text{iso}} A_{\text{con}} \langle S_\epsilon S_\tau \rangle$	6	$\sigma_{\text{con},3}$	$\mathcal{O}(\alpha^4)$	0	0, 2
$\Delta g_{\text{iso}} \sum_b A_{b\tau}^{\text{dip}} \langle S_\epsilon S_b \rangle$	7	$\sigma_{\text{dip},3}$	$\mathcal{O}(\alpha^4)$	2	0, 2, 1
$A_{\text{con}} \sum_a \Delta \tilde{g}_{\epsilon a} \langle S_a S_\tau \rangle$	8	$\sigma_{\text{c,aniso}}$	$\mathcal{O}(\alpha^4)$	2, 1	0, 2, 1
$\sum_{ab} \Delta \tilde{g}_{\epsilon a} A_{b\tau}^{\text{dip}} \langle S_a S_b \rangle$	9	$\sigma_{\text{pc}}$	$\mathcal{O}(\alpha^4)$	0, 2, 1	0, 2, 1

<sup>a</sup> Contributions with rank 0, 2 and 1 correspond to the isotropic shielding constant, anisotropic symmetric terms and anisotropic antisymmetric terms, respectively.

Table ESI12: Physical contributions to the isotropic nuclear shieldings for  $[\text{Tp}_2\text{Fe}]^+$ . Computational details as in Table ESI8.

Level of theory/Term no.	H3	H4	H5	BH	C3	C4	C5	B	N1	N2
cas(5,5), mDKS										
$\sigma_{\text{orb}}$	27.0	25.2	22.7	24.7	43.3	73.7	42.9	107.0	9.3	-0.6
1 + 3	20.1	11.2	29.8	-3.6	33.6	103.2	-3.5	-10.2	336.3	2866.2
2 + 4	0.0	0.0	0.0	0.0	0.0	0.0	0.0	0.0	0.0	0.0
5	0.0	0.0	0.0	0.0	0.0	0.0	0.0	0.0	0.0	0.0
6	-0.4	-0.2	-0.6	0.1	-0.7	-2.1	0.1	0.2	-6.9	-59.1
7	0.0	0.0	0.0	0.0	0.0	0.0	0.0	0.0	0.0	0.0
8	0.0	0.0	0.0	0.0	0.0	0.0	0.0	0.0	0.0	0.0
9	36.5	5.7	-18.1	-30.9	77.4	17.2	55.3	-86.3	-58.3	-5.7
$\sigma_{\text{tot}}$	83.1	41.8	33.8	-9.7	153.7	192.0	94.7	10.7	280.2	2800.8
cas(9,12), mDKS (PBE)										
$\sigma_{\text{orb}}$	27.0	25.2	22.7	24.7	43.3	73.7	42.9	107.0	9.3	-0.6
1 + 3	16.6	18.6	33.5	-2.0	94.5	73.1	-14.2	-3.3	320.8	1874.4
2 + 4	0.0	0.0	0.0	0.0	0.0	0.0	0.0	0.0	0.0	0.0
5	0.0	0.0	0.0	0.0	0.0	0.0	0.0	0.0	0.0	0.0
6	-1.4	-1.6	-2.8	0.2	-8.0	-6.2	1.2	0.3	-27.0	-157.8
7	0.0	0.0	0.0	0.0	0.0	0.0	0.0	0.0	0.0	0.0
8	0.0	0.0	0.0	0.0	0.0	0.0	0.0	0.0	0.0	0.0
9	33.6	8.8	-21.2	-28.8	76.6	47.3	95.8	-78.6	-47.0	88.5
$\sigma_{\text{tot}}$	75.8	50.9	32.2	-5.9	206.4	187.9	125.7	25.4	256.0	1804.5
cas(9,12), mDKS (PBE-25)										
$\sigma_{\text{orb}}$	27.0	25.2	22.7	24.7	43.3	73.7	42.9	107.0	9.3	-0.6
1 + 3	20.1	11.2	29.8	-3.6	33.6	103.2	-3.5	-10.2	336.3	2866.2
2 + 4	0.0	0.0	0.0	0.0	0.0	0.0	0.0	0.0	0.0	0.0
5	0.0	0.0	0.0	0.0	0.0	0.0	0.0	0.0	0.0	0.0
6	-1.7	-0.9	-2.5	0.3	-2.8	-8.7	0.3	0.9	-28.3	-241.4
7	0.0	0.0	0.0	0.0	0.0	0.0	0.0	0.0	0.0	0.0
8	0.0	0.0	0.0	0.0	0.0	0.0	0.0	0.0	0.0	0.0
9	37.3	5.8	-18.5	-31.6	79.7	17.7	57.2	-88.3	-59.7	-5.6
$\sigma_{\text{tot}}$	82.7	41.2	31.5	-10.2	153.8	185.9	96.8	9.4	257.5	2618.7
cas(9,12), mDKS (PBE-40)										
$\sigma_{\text{orb}}$	27.0	25.2	22.7	24.7	43.3	73.7	42.9	107.0	9.3	-0.6
1 + 3	23.2	7.8	30.9	-4.4	-14.7	118.9	-12.2	-15.1	354.6	3328.2
2 + 4	0.0	0.0	0.0	0.0	0.0	0.0	0.0	0.0	0.0	0.0
5	0.0	0.0	0.0	0.0	0.0	0.0	0.0	0.0	0.0	0.0
6	-2.0	-0.7	-2.6	0.4	1.2	-10.0	1.0	1.3	-29.9	-280.3
7	0.0	0.0	0.0	0.0	0.0	0.0	0.0	0.0	0.0	0.0
8	0.0	0.0	0.0	0.0	0.0	0.0	0.0	0.0	0.0	0.0
9	38.7	5.0	-18.6	-32.9	83.9	7.9	49.8	-92.5	-64.8	-37.1
$\sigma_{\text{tot}}$	87.0	37.3	32.4	-12.3	113.8	190.5	81.5	0.7	269.2	3010.3
cas(9,12), mDKS (PBE-100)										
$\sigma_{\text{orb}}$	27.0	25.2	22.7	24.7	43.3	73.7	42.9	107.0	9.3	-0.6
1 + 3	42.2	-16.1	58.8	1.9	-361.4	271.1	-223.3	-45.4	638.8	3807.1
2 + 4	0.0	0.0	0.0	0.0	0.0	0.0	0.0	0.0	0.0	0.0
5	0.0	0.0	0.0	0.0	0.0	0.0	0.0	0.0	0.0	0.0
6	-3.6	1.4	-5.0	-0.2	30.4	-22.8	18.8	3.8	-53.8	-320.6
7	0.0	0.0	0.0	0.0	0.0	0.0	0.0	0.0	0.0	0.0
8	0.0	0.0	0.0	0.0	0.0	0.0	0.0	0.0	0.0	0.0
9	28.9	3.5	-29.7	-33.5	157.5	-75.1	108.8	-89.6	-182.5	-469.7
$\sigma_{\text{tot}}$	94.5	14.0	46.8	-7.1	-130.2	246.8	-52.8	-24.1	411.7	3016.3
cas(9,12), DKH										
$\sigma_{\text{orb}}$	27.0	25.2	22.7	24.7	43.3	73.7	42.9	107.0	9.3	-0.6
1 + 3	17.3	11.2	32.1	-1.1	19.8	104.6	-3.1	-3.9	351.3	3003.0
2 + 4	0.0	0.0	0.0	0.0	0.0	0.0	0.0	0.0	0.0	0.0
5	0.0	0.0	0.0	0.0	0.0	0.0	0.0	0.0	0.0	0.0
6	-1.5	-0.9	-2.7	0.1	-1.7	-8.8	0.3	0.3	-29.6	-252.9
7	0.0	0.0	0.0	0.0	0.0	0.0	0.0	0.0	0.0	0.0

8	0.0	0.0	0.0	0.0	0.0	0.0	0.0	0.0	0.0	0.0
9	32.8	5.5	-17.6	-28.4	65.7	16.1	59.9	-80.0	-57.4	-13.1
$\sigma_{\text{tot}}$	75.7	40.9	34.4	-4.8	127.2	185.5	99.9	23.4	273.6	2736.5
cas(9,12), DKH + [PF <sub>6</sub> ] <sup>-</sup>										
$\sigma_{\text{orb}}$	27.0	25.2	22.7	24.7	43.3	73.7	42.9	107.0	9.3	-0.6
1 + 3	16.5	13.0	33.1	-1.0	31.8	93.9	-9.2	-4.8	350.0	2845.7
2 + 4	0.0	0.0	0.0	0.0	0.0	0.0	0.0	0.0	0.0	0.0
5	0.0	0.0	0.0	0.0	0.0	0.0	0.0	0.0	0.0	0.0
6	-1.4	-1.1	-2.8	0.1	-2.7	-7.9	0.8	0.4	-29.5	-239.6
7	0.0	0.0	0.0	0.0	0.0	0.0	0.0	0.0	0.0	0.0
8	0.0	0.0	0.0	0.0	0.0	0.0	0.0	0.0	0.0	0.0
9	31.6	6.3	-17.5	-26.4	57.8	20.2	57.5	-74.8	-54.6	-5.8
$\sigma_{\text{tot}}$	73.7	43.3	35.5	-2.6	130.2	179.9	92.0	27.8	275.2	2599.7
cas(9,12), DKH + C-PCM										
$\sigma_{\text{orb}}$	27.0	25.2	22.7	24.7	43.3	73.7	42.9	107.0	-	-
1 + 3	17.8	11.1	31.8	-1.2	19.1	105.4	-2.4	-4.3	-	-
2 + 4	0.0	0.0	0.0	0.0	0.0	0.0	0.0	0.0	-	-
5	0.0	0.0	0.0	0.0	0.0	0.0	0.0	0.0	-	-
6	-1.5	-0.9	-2.7	0.1	-1.6	-8.9	0.2	0.4	-	-
7	0.0	0.0	0.0	0.0	0.0	0.0	0.0	0.0	-	-
8	0.0	0.0	0.0	0.0	0.0	0.0	0.0	0.0	-	-
9	32.8	5.4	-17.5	-28.4	67.1	15.7	58.9	-80.1	-	-
$\sigma_{\text{tot}}$	76.1	40.7	34.3	-4.8	127.9	185.9	99.6	23.0	-	-
cas(9,12), DKH + C-PCM <sup>a</sup>										
$\sigma_{\text{orb}}$	27.0	25.2	22.7	24.7	43.3	73.7	42.9	107.0	9.3	-0.6
1 + 3	17.9	11.1	32.1	-1.1	18.3	105.5	-5.0	-4.3	352.8	2984.2
2 + 4	0.0	0.0	0.0	0.0	0.0	0.0	0.0	0.0	0.0	0.0
5	0.0	0.0	0.0	0.0	0.0	0.0	0.0	0.0	0.0	0.0
6	-1.5	-0.9	-2.7	0.1	-1.5	-8.9	0.4	0.4	-29.7	-251.3
7	0.0	0.0	0.0	0.0	0.0	0.0	0.0	0.0	0.0	0.0
8	0.0	0.0	0.0	0.0	0.0	0.0	0.0	0.0	0.0	0.0
9	32.2	5.8	-18.0	-28.2	58.0	14.3	47.8	-79.7	-55.9	-14.5
$\sigma_{\text{tot}}$	75.6	41.1	34.1	-4.6	118.1	184.6	86.1	23.4	276.4	2717.8
cas(9,12), DKH + 12 acetones										
$\sigma_{\text{orb}}$	27.0	25.2	22.7	24.7	43.3	73.7	42.9	107.0	9.3	-0.6
1 + 3	18.0	10.4	33.5	-1.2	14.9	114.9	-18.2	-6.3	364.6	3043.0
2 + 4	0.0	0.0	0.0	0.0	0.0	0.0	0.0	0.0	0.0	0.0
5	0.0	0.0	0.0	0.0	0.0	0.0	0.0	0.0	0.0	0.0
6	-1.5	-0.9	-2.8	0.1	-1.3	-9.7	1.5	0.5	-30.7	-256.3
7	0.0	0.0	0.0	0.0	0.0	0.0	0.0	0.0	0.0	0.0
8	0.0	0.0	0.0	0.0	0.0	0.0	0.0	0.0	0.0	0.0
9	30.1	5.0	-16.9	-26.4	63.3	11.6	56.3	-74.5	-52.7	-17.8
$\sigma_{\text{tot}}$	73.6	39.7	36.5	-2.8	120.3	190.4	82.4	26.8	290.5	2768.4
cas(9,12), DLPNO-CCSD										
$\sigma_{\text{orb}}$	27.0	25.2	22.7	24.7	43.3	73.7	42.9	107.0	9.3	-0.6
1 + 3	16.8	5.3	19.3	-0.9	1.6	101.8	-19.3	0.8	194.0	3198.0
2 + 4	0.0	0.0	0.0	0.0	0.0	0.0	0.0	0.0	0.0	0.0
5	0.0	0.0	0.0	0.0	0.0	0.0	0.0	0.0	0.0	0.0
6	-1.4	-0.4	-1.6	0.1	-0.1	-8.6	1.6	-0.1	-16.3	-269.3
7	0.0	0.0	0.0	0.0	0.0	0.0	0.0	0.0	0.0	0.0
8	0.0	0.0	0.0	0.0	0.0	0.0	0.0	0.0	0.0	0.0
9	33.9	4.2	-15.1	-29.6	69.8	5.2	27.0	-81.9	-65.8	-27.8
$\sigma_{\text{tot}}$	76.3	34.2	25.3	-5.8	114.5	172.1	52.2	25.8	121.2	2900.3

<sup>a</sup> COSMO-optimised geometry and Acetone-d<sub>6</sub> solvent ( $\epsilon = 20.7$ ) used in HFC calculation.

Table ESI13: Physical contributions to the isotropic nuclear shieldings for the high-spin ( $S = 2$ ) state of  $\text{Tp}_2\text{Fe}$  at 455 K. Computational details otherwise as in Table ESI14.

Level of theory/Term no.	H3	H4	H5	BH	C3	C4	C5	B	N1	N2
cas(6,5), mDKS										
$\sigma_{\text{orb}}$	22.8	25.3	24.5	28.1	40.6	79.8	52.6	115.3	16.1	-41.9
1 + 3	-12.8	-27.4	-8.4	10.5	-421.4	-279.2	-443.9	42.2	-26	-13724.4
2 + 4	-4.8	-0.4	2.1	4.8	-5.6	0.1	1.3	11.9	10.7	5.5
5	0.0	0.0	0.0	0.0	0.0	0.0	0.0	0.0	0.0	0.0
6	-0.4	-0.9	-0.3	0.4	-14.6	-9.7	-15.4	1.5	-0.9	-475.8
7	-0.2	0.0	0.1	0.2	-0.2	0.0	0.0	0.4	0.4	0.2
8	0.0	0.0	0.0	0.0	-0.3	-0.2	-0.3	0.0	0.0	-10.2
9	-4.8	-0.4	2.1	4.8	-5.5	0.1	1.3	11.9	10.6	5.5
$\sigma_{\text{tot}}$	-0.1	-3.8	20.1	48.7	-407.0	-209.0	-404.4	183.1	10.9	-14241.1
cas(10,12), mDKS (PBE)										
$\sigma_{\text{orb}}$	22.8	25.3	24.5	28.1	40.6	79.8	52.6	115.3	16.1	-41.9
1 + 3	-21.5	-38.1	-18.4	12.0	-544.4	-419.8	-627.9	58.1	-182.2	-16292.6
2 + 4	-4.4	-0.4	2.0	4.5	-5.8	0.0	0.6	10.8	10.4	3.7
5	0.0	0.0	0.0	0.0	0.0	0.0	0.0	0.0	0.0	0.0
6	-0.7	-1.3	-0.6	0.4	-18.5	-14.3	-21.3	2.0	-6.2	-553.8
7	-0.1	0.0	0.1	0.2	-0.2	0.0	0.0	0.4	0.4	0.1
8	0.0	0.0	0.0	0.0	-0.4	-0.3	-0.4	0.0	-0.1	-10.8
9	-4.4	-0.4	2.0	4.5	-5.8	0.0	0.6	10.8	10.4	3.7
$\sigma_{\text{tot}}$	-8.3	-14.9	9.6	49.6	-534.5	-354.6	-595.9	197.4	-151.2	-16891.7
cas(10,12), mDKS (PBE-25)										
$\sigma_{\text{orb}}$	22.8	25.3	24.5	28.1	40.6	79.8	52.6	115.3	16.1	-41.9
1 + 3	-12.8	-27.4	-8.4	10.5	-421.4	-279.2	-443.9	42.2	-26.0	-13724.6
2 + 4	-4.5	-0.3	2.0	4.5	-5.3	0.1	1.2	11.3	10.1	5.2
5	0.0	0.0	0.0	0.0	0.0	0.0	0.0	0.0	0.0	0.0
6	-0.4	-0.9	-0.3	0.4	-14.3	-9.5	-15.1	1.4	-0.9	-466.5
7	-0.2	0.0	0.1	0.2	-0.2	0.0	0.0	0.4	0.3	0.2
8	0.0	0.0	0.0	0.0	-0.3	-0.2	-0.3	0.0	0.0	-9.1
9	-4.5	-0.3	2.0	4.5	-5.3	0.1	1.2	11.3	10.1	5.2
$\sigma_{\text{tot}}$	0.4	-3.8	19.9	48.2	-406.1	-208.8	-404.2	181.9	9.8	-14231.6
cas(10,12), mDKS (PBE-40)										
$\sigma_{\text{orb}}$	22.8	25.3	24.5	28.1	40.6	79.8	52.6	115.3	16.1	-41.9
1 + 3	-9.9	-24.1	-4.4	10.3	-374.0	-226.8	-381.2	34.5	31.7	-12582.5
2 + 4	-4.6	-0.3	2.0	4.6	-5.1	0.1	1.4	11.4	10.0	5.2
5	0.0	0.0	0.0	0.0	0.0	0.0	0.0	0.0	0.0	0.0
6	-0.3	-0.8	-0.2	0.4	-12.7	-7.7	-13.0	1.2	1.1	-427.7
7	-0.2	0.0	0.1	0.2	-0.2	0.0	0.0	0.4	0.3	0.2
8	0.0	0.0	0.0	0.0	-0.2	-0.2	-0.3	0.0	0.0	-8.4
9	-4.6	-0.3	2.0	4.6	-5.1	0.1	1.4	11.4	10.0	5.2
$\sigma_{\text{tot}}$	3.3	-0.4	23.9	48.1	-356.6	-154.6	-339.1	174.2	69.3	-13049.9
cas(10,12), mDKS (PBE-100)										
$\sigma_{\text{orb}}$	22.8	25.3	24.5	28.1	40.6	79.8	52.6	115.3	16.1	-41.9
1 + 3	-3.7	-21.2	6.8	11.9	-280.5	-101.4	-283.4	7.0	213.2	-10055.8
2 + 4	-4.7	-0.3	2.0	4.6	-4.8	0.3	1.5	11.8	10.2	4.9
5	0.0	0.0	0.0	0.0	0.0	0.0	0.0	0.0	0.0	0.0
6	-0.1	-0.7	0.2	0.4	-9.5	-3.4	-9.6	0.2	7.2	-341.8
7	-0.2	0.0	0.1	0.2	-0.2	0.0	0.1	0.4	0.3	0.2
8	0.0	0.0	0.0	0.0	-0.2	-0.1	-0.2	0.0	0.1	-6.7
9	-4.7	-0.3	2.0	4.6	-4.8	0.3	1.5	11.8	10.2	4.9
$\sigma_{\text{tot}}$	9.4	2.7	35.6	49.8	-259.3	-24.5	-237.5	146.5	257.4	-10436.2
cas(10,12), DKH										
$\sigma_{\text{orb}}$	22.8	25.3	24.5	28.1	40.6	79.8	52.6	115.3	16.1	-41.9
1 + 3	-10.2	-27.1	-9.4	7.8	-417.3	-278.5	-447.6	34.7	-39.7	-13753.7
2 + 4	-4.5	-0.3	2.0	4.5	-5.2	0.1	1.2	11.2	9.9	5.9
5	0.0	0.0	0.0	0.0	0.0	0.0	0.0	0.0	0.0	0.0
6	-0.3	-0.9	-0.3	0.3	-14.2	-9.5	-15.2	1.2	-1.4	-467.5
7	-0.2	0.0	0.1	0.2	-0.2	0.0	0.0	0.4	0.3	0.2

8	0.0	0.0	0.0	0.0	-0.3	-0.2	-0.3	0.0	0.0	-9.1
9	-4.5	-0.3	2.0	4.5	-5.2	0.1	1.2	11.2	9.9	5.9
$\sigma_{\text{tot}}$	3.1	-3.5	18.8	45.4	-401.6	-208.1	-408.2	174.0	-4.8	-14260.1
cas(10,12), DKH + C-PCM										
$\sigma_{\text{orb}}$	22.8	25.3	24.5	28.1	40.6	79.8	52.6	115.3	16.1	-
1 + 3	-10.0	-27.1	-9.5	7.8	-419.6	-274.6	-437.8	34.6	-41.2	-
2 + 4	-4.5	-0.3	2.0	4.5	-5.2	0.1	1.2	11.2	9.9	-
5	0.0	0.0	0.0	0.0	0.0	0.0	0.0	0.0	0.0	-
6	-0.3	-0.9	-0.3	0.3	-14.3	-9.3	-14.9	1.2	-1.4	-
7	-0.2	0.0	0.1	0.2	-0.2	0.0	0.0	0.4	0.3	-
8	0.0	0.0	0.0	0.0	-0.3	-0.2	-0.3	0.0	0.0	-
9	-4.5	-0.3	2.0	4.5	-5.2	0.1	1.2	11.2	9.9	-
$\sigma_{\text{tot}}$	3.4	-3.5	18.7	45.4	-404.0	-204.1	-397.9	173.9	-6.3	-
cas(10,12), DLPNO-CCSD										
$\sigma_{\text{orb}}$	22.8	25.3	24.5	28.1	40.6	79.8	52.6	115.3	16.1	-41.9
1 + 3	-5.8	-13.8	-5.2	7.7	-343.5	-180.8	-259.0	26.5	-52.0	-11465.1
2 + 4	-4.6	-0.3	1.9	4.6	-4.3	0.0	2.1	11.6	9.5	4.9
5	0.0	0.0	0.0	0.0	0.0	0.0	0.0	0.0	0.0	0.0
6	-0.2	-0.5	-0.2	0.3	-11.7	-6.1	-8.8	0.9	-1.8	-389.7
7	-0.2	0.0	0.1	0.2	-0.1	0.0	0.1	0.4	0.3	0.2
8	0.0	0.0	0.0	0.0	-0.2	-0.1	-0.2	0.0	0.0	-7.6
9	-4.6	-0.3	1.9	4.6	-4.3	0.0	2.1	11.6	9.6	4.9
$\sigma_{\text{tot}}$	7.3	10.3	23.0	45.4	-323.6	-107.2	-211.2	166.2	-18.2	-11894.4

# Full numerical pNMR results for $\text{Tp}_2\text{Fe}$

Table ESI14: Experimental and computational  $^1\text{H}$  NMR chemical shifts (ppm) for  $\text{Tp}_2\text{Fe}$  as well as fitted enthalpy gaps  $\Delta H$  (kJ/mol) and entropy gaps  $\Delta S$  [J/(Kmol)]. For the individual  $^1\text{H}$  temperature series fits, ranges of  $\Delta H$  and  $\Delta S$  as well as their average values  $\Delta H_{\text{avg}}$  and  $\Delta S_{\text{avg}}$  are given. Where no unique  $\Delta H$  and  $\Delta S$  were obtained, those values were excluded from the averages. The Gibbs free energy gap  $\Delta G = \Delta H - T\Delta S$  (kJ/mol) is calculated at room temperature (298 K). High-spin ( $S = 2$ ) and low-spin ( $S = 0$ ) computational nuclear shieldings (ppm) prior to fitting are included for completeness. Functional PBE-25 unless indicated otherwise. ZFS and  $g$ -tensor calculated at the NEVPT2 level based on the indicated CASSCF wavefunction. Geometry optimised *in vacuo* was used in all calculations. Temperature for  $^1\text{H}$ : 290 K, except in the temperature series.

Wavefunction, HFC level	H3	H4	H5	BH	$\Delta H$	$\Delta S$	$\Delta H_{\text{avg}}$	$\Delta S_{\text{avg}}$	$\Delta G$
exptl	13.0 <sup>2,3</sup>	12.9 <sup>2,3</sup>	8.1 <sup>2,3</sup>	-2.7 <sup>2,3</sup>	16.1 <sup>1</sup> /24 <sup>2</sup>	47.7 <sup>1</sup> /70 <sup>2</sup>			
Global $^1\text{H}$ temperature series fit									
cas(6,5), mDKS	15.3	15.5	9.1	-2.0	23.5	69.2			2.9
cas(10,12), mDKS (PBE)	16.6	17.6	11.8	-1.6	15.3	40.0			3.4
cas(10,12), mDKS (PBE-25)	15.1	15.5	9.2	-1.8	24.0	71.1			2.8
cas(10,12), mDKS (PBE-40)	14.0	14.3	7.9	-1.6	29.5	89.8			2.7
cas(10,12), mDKS (PBE-100)	11.4	12.5	4.0	-2.4	29.5	89.4			2.9
cas(10,12), DKH	14.1	15.3	9.5	-0.8	27.1	81.6			2.8
cas(10,12), DKH + C-PCM <sup>a</sup>	14.0	15.2	9.5	-0.8	27.3	82.1			2.8
cas(10,12), DLPNO-CCSD	13.4	11.5	8.2	-1.5	48.1	154.8			2.0
Individual $^1\text{H}$ temperature series fits									
cas(6,5), mDKS	15.1	14.9	8.4	-2.1	19.8...37.2	42.6...116.6	24.7	68.9	4.2
cas(10,12), mDKS (PBE)	16.3	16.4	8.4	-2.4	14.1...34.5	19.3...107.2	20.0	49.8	5.2
cas(10,12), mDKS (PBE-25)	14.9	14.9	8.4	-1.9	20.4...38.8	41.8...122.2	25.3	70.7	4.2
cas(10,12), mDKS (PBE-40)	13.9	13.9	8.3 <sup>b</sup>	-1.9	25.8...39.2	76.9...123.5	30.4	92.7	2.8
cas(10,12), mDKS (PBE-100)	12.3	12.5	7.7 <sup>b</sup>	-2.7	33.0...48.3	101.7...155.9	38.6	121.5	2.4
cas(10,12), DKH	13.9	14.8	8.4	-1.5	20.7...47.7	38.8...153.6	28.8	82.4	4.2
cas(10,12), DKH + C-PCM <sup>a</sup>	13.8	14.8	8.4	-1.5	20.7...47.6	38.4...153.2	28.9	82.7	4.3
cas(10,12), DLPNO-CCSD <sup>c</sup>									
Global all data fit									
cas(6,5), mDKS	10.3	10.1	8.6	2.5	34.8	99.6			5.1
cas(10,12), mDKS (PBE)	10.6	10.7	9.6	2.7	24.9	64.0			5.8
cas(10,12), mDKS (PBE-25)	10.2	10.1	8.7	2.6	35.7	102.5			5.2
cas(10,12), mDKS (PBE-40)	9.6	9.4	8.2	2.9	46.4	138.8			5.0
cas(10,12), mDKS (PBE-100)	9.9	10.5	5.1	-0.2	39.2	119.0			3.7
cas(10,12), DKH	9.6	9.8	8.7	3.1	40.3	117.8			5.2
cas(10,12), DKH + C-PCM <sup>a</sup>	9.6	9.8	8.8	3.1	40.3	117.7			5.2
cas(10,12), DLPNO-CCSD	9.1	8.2	8.3	3.2	63.2	196.5			4.6
Experimental $\Delta H$ and $\Delta S$ (Ref. <sup>1</sup> )									
cas(6,5), mDKS	18.9	19.4	9.5	-5.3					
cas(10,12), mDKS (PBE)	22.3	24.2	14.0	-5.7					
cas(10,12), mDKS (PBE-25)	18.6	19.4	9.6	-5.0					
cas(10,12), mDKS (PBE-40)	17.3	17.9	7.8	-4.9					
cas(10,12), mDKS (PBE-100)	14.0	15.9	2.1	-6.3					
cas(10,12), DKH	17.3	19.3	10.0	-3.7					
cas(10,12), DKH + C-PCM <sup>a</sup>	17.2	19.3	10.1	-3.8					
cas(10,12), DLPNO-CCSD	15.5	13.2	8.2	-3.8					
Experimental $\Delta H$ and $\Delta S$ (Ref. <sup>2</sup> )									
cas(6,5), mDKS	14.5	14.7	9.0	-1.3					
cas(10,12), mDKS (PBE)	16.6	17.7	11.8	-1.6					
cas(10,12), mDKS (PBE-25)	14.3	14.6	9.1	-1.1					
cas(10,12), mDKS (PBE-40)	13.5	13.7	8.0	-1.1					
cas(10,12), mDKS (PBE-100)	11.2	12.2	4.1	-2.2					
cas(10,12), DKH	13.5	14.6	9.4	-0.3					
cas(10,12), DKH + C-PCM <sup>a</sup>	13.5	14.6	9.4	-0.3					
cas(10,12), DLPNO-CCSD	12.4	10.7	8.3	-0.4					
High-spin ( $S = 2$ ) shieldings									
cas(6,5), mDKS	-17.4	-20.7	19.4	64.7					
cas(10,12), mDKS (PBE)	-29.9	-38.2	2.9	65.8					
cas(10,12), mDKS (PBE-25)	-16.4	-20.6	19.0	63.6					

cas(10,12), mDKS (PBE-40)	-11.9	-15.3	25.4	63.5
cas(10,12), mDKS (PBE-100)	-2.3	-10.4	43.6	66.3
cas(10,12), DKH	-12.0	-20.2	17.3	59.2
cas(10,12), DKH + C-PCM <sup>a</sup>	-11.7	-20.2	17.1	59.3
cas(10,12), DLPNO-CCSD	-5.6	1.4	23.8	59.3
Low-spin $S = 0$ shieldings	24.8	25.3	23.5	26.3

<sup>a</sup> Chloroform-d ( $\epsilon = 4.81$ ).

<sup>b</sup> Fitted  $\Delta H$  and  $\Delta S$  dependent on initial values, but unambiguous shieldings were still obtained.

<sup>c</sup> Fitted  $\Delta H$  and  $\Delta S$  dependent on initial values, no unambiguous shieldings; omitted from results.



Table ESI15: As Table ESI14 but for  $^{13}\text{C}$ ,  $^{11}\text{B}$  and  $^{14}\text{N}$ . Fitted  $\Delta H$  and  $\Delta S$  in Table ESI14. Temperature for  $^{13}\text{C}$ : 305 K;  $^{11}\text{B}$  and  $^{14}\text{N}$ : 298 K.

Wavefunction, HFC level	C3	C4	C5	B	N1	N2
exptl <sup>2,3</sup>	266	168	229	-26.4	-126	-
Global $^1\text{H}$ temperature series fit						
cas(6,5), mDKS	341.3	231.9	332.5	-37.5	-143.9	5127.8
cas(10,12), mDKS (PBE)	343.1	253.2	355.4	-42.6	-67.7	5142.8
cas(10,12), mDKS (PBE-25)	342.4	232.8	333.9	-37.0	-143.4	5148.9
cas(10,12), mDKS (PBE-40)	333.2	217.6	317.8	-31.7	-181.3	4804.4
cas(10,12), mDKS (PBE-100)	276.6	149.5	259.5	-34.6	-157.1	3751.0
cas(10,12), DKH	345.5	235.8	340.8	-34.3	-137.9	5191.5
cas(10,12), DKH + C-PCM <sup>a</sup>	346.6	234.1	336.4	-34.2	-137.4	-
cas(10,12), DLPNO-CCSD	378.0	225.9	302.2	-37.8	-130.8	5573.7
Individual $^1\text{H}$ temperature series fits						
cas(6,5), mDKS	279.0	191.9	269.4	-27.6	-142.5	3303.2
cas(10,12), mDKS (PBE)	259.9	190.6	262.2	-29.8	-89.2	2760.1
cas(10,12), mDKS (PBE-25)	278.0	191.4	268.6	-27.1	-142.2	3266.6
cas(10,12), mDKS (PBE-40)	333.8	217.9	318.4	-31.6	-181.3	4792.8
cas(10,12), mDKS (PBE-100)	303.3	158.7	285.1	-36.8	-171.3	4329.6
cas(10,12), DKH	276.6	191.1	269.6	-24.7	-138.7	3177.5
cas(10,12), DKH + C-PCM <sup>a</sup>	276.3	189.3	265.7	-24.5	-138.4	-
cas(10,12), DLPNO-CCSD <sup>b</sup>						
Global all data fit						
cas(6,5), mDKS	251.7	174.4	241.8	-22.4	-141.8	2337.4
cas(10,12), mDKS (PBE)	241.6	176.8	241.7	-26.8	-94.3	2190.9
cas(10,12), mDKS (PBE-25)	251.6	174.4	241.9	-22.0	-141.6	2320.9
cas(10,12), mDKS (PBE-40)	252.1	169.9	238.7	-17.9	-167.3	2147.9
cas(10,12), mDKS (PBE-100)	256.1	142.4	240.0	-31.3	-136.0	2899.6
cas(10,12), DKH	250.7	174.3	242.8	-20.3	-139.1	2235.3
cas(10,12), DKH + C-PCM <sup>a</sup>	252.3	174.1	241.6	-20.4	-138.8	-
cas(10,12), DLPNO-CCSD	269.7	170.5	224.9	-21.4	-136.1	2311.4
Experimental $\Delta H$ and $\Delta S$ (Ref. <sup>1</sup> )						
cas(6,5), mDKS	387.0	261.3	378.7	-46.6	-145.1	6803.1
cas(10,12), mDKS (PBE)	450.2	334.0	475.5	-58.6	-40.9	8117.7
cas(10,12), mDKS (PBE-25)	386.5	261.2	378.7	-45.8	-144.4	6798.5
cas(10,12), mDKS (PBE-40)	362.5	234.8	346.4	-39.0	-188.7	6208.5
cas(10,12), mDKS (PBE-100)	303.6	158.8	285.4	-39.5	-188.6	5029.2
cas(10,12), DKH	384.1	260.9	380.7	-42.0	-137.3	6812.2
cas(10,12), DKH + C-PCM <sup>a</sup>	385.4	258.7	375.3	-41.9	-136.6	-
cas(10,12), DLPNO-CCSD	343.0	208.0	277.2	-38.3	-130.6	5662.1
Experimental $\Delta H$ and $\Delta S$ (Ref. <sup>2</sup> )						
cas(6,5), mDKS	326.0	222.1	317.0	-35.0	-143.5	4662.7
cas(10,12), mDKS (PBE)	371.8	274.9	387.6	-45.0	-63.8	5577.6
cas(10,12), mDKS (PBE-25)	325.6	222.0	316.9	-34.4	-143.1	4659.5
cas(10,12), mDKS (PBE-40)	308.4	203.0	293.6	-28.8	-178.4	4247.6
cas(10,12), mDKS (PBE-100)	262.8	144.7	246.4	-33.5	-149.9	3462.3
cas(10,12), DKH	323.9	221.8	318.4	-31.8	-138.1	4668.9
cas(10,12), DKH + C-PCM <sup>a</sup>	324.8	220.2	314.4	-31.7	-137.6	-
cas(10,12), DLPNO-CCSD	293.4	182.6	241.8	-29.3	-133.5	3875.4
High-spin ( $S = 2$ ) shieldings						
cas(6,5), mDKS	-631.2	-351.0	-628.3	228.4	16.7	-21720.4
cas(10,12), mDKS (PBE)	-821.7	-568.4	-914.4	249.4	-231.1	-25769.1
cas(10,12), mDKS (PBE-25)	-629.7	-350.7	-628.1	226.0	14.6	-21705.9
cas(10,12), mDKS (PBE-40)	-555.8	-269.8	-530.8	214.4	105.4	-19901.5
cas(10,12), mDKS (PBE-100)	-410.3	-75.6	-379.1	172.4	392.7	-15910.5
cas(10,12), DKH	-623.0	-349.7	-634.0	213.9	-7.9	-21748.9
cas(10,12), DKH + C-PCM <sup>a</sup>	-626.6	-343.7	-618.7	213.7	-10.1	-
cas(10,12), DLPNO-CCSD	-505.9	-199.2	-339.5	202.4	-28.7	-18137.2
Low-spin $S = 0$ shieldings						
	36.0	77.9	47.2	111.1	0.7	-37.9

<sup>a</sup> Toluene ( $\epsilon = 2.38$ ).

<sup>b</sup> Fitted  $\Delta H$  and  $\Delta S$  dependent on initial values, no unambiguous shieldings; omitted from results.

## NMR shifts with alternative experimental $\Delta H$ and $\Delta S$ (Ref.<sup>1</sup>) for $\text{Tp}_2\text{Fe}$

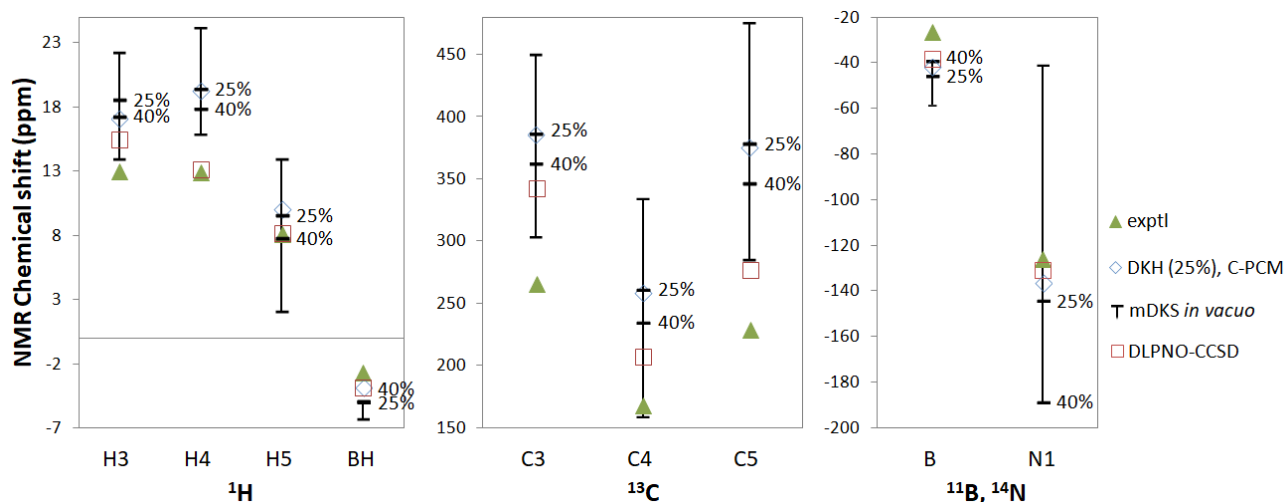


Figure ESI6: Experimental<sup>2,3</sup> and computational NMR chemical shifts for  $\text{Tp}_2\text{Fe}$  with experimental parameters  $\Delta H = 16.1$  kJ/mol and  $\Delta S = 47.7$  J/(Kmol) (Ref.<sup>1</sup>). Bars indicate the range of *in vacuo* mDKS results for hyperfine coupling tensors obtained with hybrid, PBE0-based exchange-correlation functionals with different exact exchange admixtures. Temperature for  $^1\text{H}$ : 290 K;  $^{13}\text{C}$ : 305 K;  $^{11}\text{B}$  and  $^{14}\text{N}$ : 298 K.

## Energetics of the spin-crossover system $\text{Tp}_2\text{Fe}$

Table ESI16: Energy gap (kJ/mol) between the high-spin ( $S = 2$ ) and low-spin ( $S = 0$ ) states of  $\text{Tp}_2\text{Fe}$  at the state-specific CASSCF/NEVPT2 and DLPNO-CCSD(T0) levels. The CASSCF wavefunctions have been calculated at cas(6,5) and cas(10,12) levels. The notation T0 refers to the "semi-canonical" perturbative triples correction approximation. Locally dense basis sets with def2-SVP on ligand atoms and def2-TZVP or def2-QZVPP on the iron atom and its immediate vicinity have been used. The calculations utilised geometries optimised for each state. The energy gaps of the triplet ( $S = 1$ ) state are included in the last three rows, calculated only with the larger basis set.

exptl	16.1 <sup>1</sup> /24 <sup>2</sup>	
Level of theory	SVP/TZVP	SVP/QZVPP
cas(6,5); CASSCF	-270.3	-264.3
cas(6,5); NEVPT2	32.2	61.2
cas(10,12); CASSCF	-163.1	-159.3
cas(10,12); NEVPT2	-22.4	13.1
DLPNO-CCSD(T0)	-7.3	14.6
cas(10,12); CASSCF <sup>a</sup>	-	22.2
cas(10,12); NEVPT2 <sup>a</sup>	-	93.6
DLPNO-CCSD(T0) <sup>a</sup>	-	93.0

<sup>a</sup> Energy gap of the triplet relative to the low-spin ground state.

## References

- [1] J. P. Jesson, S. Trofimenko and D. R. Eaton, *J. Am. Chem. Soc.*, 1967, **89**, 3158–3164.
- [2] A. Pykkönen, R. Feher, F. H. Köhler and J. Vaara, *Inorg. Chem.*, 2020, **59**, 9294–9307.
- [3] R. Feher, *dissertation*, Technische Universität München, 1996.
- [4] L. F. Chibotaru and L. Ungur, *J. Chem. Phys.*, 2012, **137**, 064112.

[5] J. Vaara, S. A. Rouf and J. Mareš, *J. Chem. Theory Comput.*, 2015, **11**, 4840–4849.